Accepted Manuscript published as JOE-22-0106.R2. Accepted for publication: 24-Aug-2022

Sustained glucagon receptor antagonism in insulin deficient high fat fed mice

Ryan A. Lafferty, Laura M. McShane, Zara J. Franklin, Peter R. Flatt, Finbarr P.M. O'Harte, Nigel Irwin*

Biomedical Sciences Research Institute, Centre for Diabetes, Ulster University, Coleraine, Northern Ireland, UK.

*Address correspondence to: Prof. Nigel Irwin, Centre for Diabetes, Ulster University, Coleraine, Northern Ireland, UK. E-mail: n.irwin@ulster.ac.uk

Short title: GCGR antagonism in insulin-deficient HFF mice

Keywords: glucagon; glucose homeostasis; insulin sensitivity; high fat fed mice, streptozotocin

Abstract

Discerning modification to the amino acid sequence of native glucagon can generate specific glucagon receptor (GCGR) antagonists, that include desHis^{1}Pro^{4}Glu^{9}-glucagon and the acylated form desHis^{1}Pro^{4}Glu^{9}(Lys^{12}PAL)-glucagon. In the current study, we have evaluated the metabolic benefits of once daily injection of these peptide-based GCGR antagonists for 18 days in insulin-resistant high fat fed (HFF) mice with streptozotocin (STZ)-induced insulin deficiency, namely HFF-STZ mice. Administration of desHis^{1}Pro^{4}Glu^{9}-glucagon moderately ($P<0.05$) decreased STZ-induced elevations of food intake. Body weight was not different between groups of HFF-STZ mice and both treatment interventions delayed ($P<0.05$) the onset of hyperglycaemia. The treatments reduced ($P<0.05$ - $P<0.001$) circulating and pancreatic glucagon, whilst desHis^{1}Pro^{4}Glu^{9}(Lys^{12}PAL)-glucagon also substantially increased ($P<0.001$) pancreatic insulin stores. Oral glucose tolerance was appreciably improved ($P<0.05$) by both antagonists, despite lack of augmentation of glucose-stimulated insulin release. Interestingly, positive effects on intraperitoneal glucose tolerance were less obvious suggesting important beneficial effects on gut function. Metabolic benefits were accompanied by decreased ($P<0.05$ - $P<0.01$) locomotor activity and increases ($P<0.001$) in energy expenditure and respiratory exchange ratio in both treatment groups. In addition, desHis^{1}Pro^{4}Glu^{9}-glucagon increased ($P<0.01$ - $P<0.001$) O_2 consumption and CO_2 production. Together, these data provide further evidence that peptidic GCGR antagonists are effective treatment options for obesity-driven forms of diabetes, even when accompanied by insulin deficiency.

Accepted Manuscript published as JOE-22-0106.R2. Accepted for publication: 24-Aug-2022

Introduction

It has been well established that abnormal elevation in circulating glucagon leads to an increase in hepatic glucose production and glycogen metabolism that contribute to hyperglycaemia in diabetes (Unger 1978). For this reason, blockade of glucagon receptor (GCGR) signalling has been widely regarded as a potential therapeutic option to help control blood glucose levels for the treatment of diabetes (Patil et al. 2020; Lafferty et al. 2021). In addition, some recent observations (Wang et al. 2021), coupled with earlier work (Okamoto et al. 2015; 2017), suggest that GCGR blockade can also promote recovery of functional beta-cell mass, with obvious additional benefits for diabetes. Indeed, there are several reports that GCGR knockout (KO) mice are more resistant to beta-cell destruction in response to islet stress (Conarello et al. 2007; Lee at al. 2012).

Various chemical approaches have been taken in an attempt to annul GCGR activity for therapeutic benefit including, small molecules (Mu et al. 2012; Guzman-Perez et al. 2013; Pettus et al. 2020), monoclonal antibodies (Kim et al. 2012; Okamoto et al. 2015; 2017) or antisense oligonucleotides (Liang et al. 2004; Morgan et al. 2019). Although all approaches possess robust glucose-lowering actions, the adverse side effect profile of each has been questioned (Patil et al. 2020; Lafferty et al. 2021). To date, it appears that peptide-based GCGR antagonists offer the best efficacy versus side effect profile (O'Harte et al. 2013; Irwin et al. 2013; McShane et al. 2014; Franklin et al. 2014; 2022). Whether this relates to composition of the compounds in question, or overall potency and degree of GCGR blockade, remains to be determined. However, a wealth of data suggests that organic peptides such as, desHis^{1}Pro^{4}Glu^{9}-glucagon, represent highly effective GCGR antagonists (O'Harte et al. 2013; Franklin et al. 2022). Indeed, other truncated glucagon-based peptides have recently been shown to yield selective, high potency, GCGR antagonists (Yang et al. 2021), supporting this as an effective approach to decrease GCGR activity. Moreover, an acylated, longer-acting, version of desHis^{1}Pro^{4}Glu^{9}-glucagon has

been described, namely desHis[1]Pro[4]Glu[9]-glucagon(Lys[12]PAL), that also effectively antagonises the GCGR (Franklin et al. 2014). This analogue has a palmitic acid covalently attached to the Lys[12] residue of desHis[1]Pro[4]Glu[9]-glucagon via a γ-glutamyl spacer molecule, delivering a significantly extended pharmacodynamic profile (O'Harte et al. 2013). Notably, our previous work fully characterises the *in vitro* and acute *in vivo* biological action profile of both desHis[1]Pro[4]Glu[9]-glucagon and desHis[1]Pro[4]Glu[9]-glucagon(Lys[12]PAL), including effects on cAMP accumulation, insulin secretion, inhibition of glucagon action, glucose disposal and islet hormone secretion (O'Harte et al. 2013; Franklin et al. 2014).

Moreover, we have also previously shown that sustained administration of desHis[1]Pro[4]Glu[9]-glucagon, or its Lys[12] acylated counterpart, can reverse aspects of genetically- and dietary-induced obesity-related diabetes in obese-diabetic (*ob/ob*) and high-fat-fed (HFF) mice, respectively (O'Harte et al. 2014). However, both these murine models of diabetes are associated with adaptive beta-cell expansion prior to development of overt diabetes. In this regard, administration of the beta-cell toxin, streptozotocin (STZ), can counter beta-cell compensation and prevent such innate adaptations (Furman 2015). Thus, HFF mice with STZ-induced compromised beta-cells are characterised by obstruction of the classical beta-cell hypertrophy in response to prolonged high fat feeding (Tanday et al. 2021). Therefore, this HFF-STZ murine model represents an ideal tool to fully explore the positive effects of peptide-based GCGR antagonists in obesity-driven forms of diabetes, where restoration of functional beta-cell mass would be highly advantageous. Notably, benefits of GCGR blockade are believed to require at least some residual beta-cell function (Damond et al. 2016), which would be the case for HFF-STZ mice (Tanday et al. 2021).

Consequently, in the current study we have investigated the impact of once-daily treatment with desHis[1]Pro[4]Glu[9]-glucagon or desHis[1]Pro[4]Glu[9]-glucagon(Lys[12]PAL) in

Accepted Manuscript published as JOE-22-0106.R2. Accepted for publication: 24-Aug-2022

HFF-STZ mice for 18 days. Effects on food and fluid intake, as well as body weight and circulating glucose were assessed at regular intervals. Metabolic status of the mice was then examined at the end of the treatment period through glucose and insulin tolerance tests. Finally, aspects of indirect calorimetry and pancreatic hormone content were also investigated. Taken together, we reveal that peptidic GCGR antagonists possess metabolic benefits following STZ-induced beta-cell insult in insulin-resistant HFF mice, that merits further investigation in terms of translation to the clinical setting.

Materials and Methods

Peptides

All peptides were synthesised by Synpeptide (Shanghai, China) at 95% purity, which was confirmed in-house by high-performance liquid chromatography (HPLC) and MALDI-TOF, as previously described (Lafferty et al. 2020).

Animals

Young male NIH Swiss mice (10-week-old; n=8) were maintained on high fat diet (45% fat, 20% protein and 25% carbohydrates; percent of total energy of 26.15 kJ/g; Special Diets Services, Essex, UK) for 12 weeks, by which stage obesity was clearly manifested. After this period, mice were administered with a single large intraperitoneal (i.p.) dose of STZ (4-hour fast, 125 mg/kg bw, dissolved in sodium citrate buffer, pH 4.5). A separate group on HFF mice that did not receive STZ injection were employed as an additional control group. Appropriate numbers of non-diabetic control mice were not available for inclusion in the current study, but the basic phenotype of HFF mice such as obesity, impaired, glucose tolerance, hyperinsulinaemia and insulin resistance were confirmed.

Chronic *in vivo* experiments

Groups (n=8) of HFF-STZ mice received once-daily i.p. injections (10:00) of saline vehicle (0.9% (w/v) NaCl), desHis^{1}Pro^{4}Glu^{9}-glucagon or desHis^{1}Pro^{4}Glu^{9}-glucagon(Lys^{12}PAL) (both at 25 nmol/kg bw) for 18 days, starting on the same day that STZ was administered. To acclimatise mice to the injection regimen, all mice received once daily i.p. injections of saline over a 6-day run in period. Mice were maintained on high (45%) fat diet throughout the experiment. At regular intervals, cumulative energy and fluid intake, body weight and non-fasting circulating glucose were assessed. At the end of the treatment period, oral and i.p. glucose tolerance (18 mmol/kg bw; i.p. or oral as appropriate; 18-h fasted) as well as insulin sensitivity (5 U/kg bovine insulin; i.p.; non-fasted) tests were conducted. Aspects of indirect calorimetry were measured using an Oxymax Comprehensive Laboratory Animal Monitoring System (CLAMS), with 18 h acclimation prior to recordings (Columbus Instruments, OH, USA). Following the acclimatisation period, O_2 consumption, CO_2 production, respiratory exchange ratio (RER), energy expenditure and locomotor activity were assessed, as described previously (O'Harte et al. 2018). All animal experiments were approved by Ulster University Animal Ethics Review Committee and conducted in accordance with the UK Animals (Scientific Procedures) Act 1986.

Biochemical analyses

Blood samples were obtained from conscious mice via the cut tip on the tail vein and blood glucose immediately measured using an Ascencia Contour blood glucose meter (Bayer Healthcare Newbury, UK). Pancreatic or plasma insulin and glucagon, as appropriate, were measured by in-house radioimmunoassay (Flatt & Bailey 1981) or commercially available ELISA (EZGLU-30K, Merck Millipore, Burlington, Massachusetts), respectively.

Statistical analyses

Accepted Manuscript published as JOE-22-0106.R2. Accepted for publication: 24-Aug-2022

Statistical tests were conducted using GraphPad PRISM software (Version 5.0). Values are expressed as mean ± SEM. Comparative analyses between groups were performed using a one-way or two-way ANOVA with Bonferroni's *post hoc* test, as appropriate. Differences were deemed significant if $P<0.05$.

Results

Effects of desHis^{1}Pro^{4}Glu^{9}-glucagon or desHis^{1}Pro^{4}Glu^{9}-glucagon(Lys^{12}PAL) on food and fluid intake, body weight, circulating glucose and glucagon in HFF-STZ mice

Food intake was significantly ($P<0.05$ - $P<0.001$) increased in all HFF mice that received STZ injection (Fig. 1A). Only treatment with desHis^{1}Pro^{4}Glu^{9}-glucagon led to reductions ($P<0.05$) of STZ-induced elevations of food intake that was evident on days 10 and 12 (Fig. 1A). Interestingly, STZ related increases ($P<0.05$ - $P<0.001$) in fluid intake were partially reversed ($P<0.05$) in desHis^{1}Pro^{4}Glu^{9}-glucagon(Lys^{12}PAL) treated mice, but not by desHis^{1}Pro^{4}Glu^{9}-glucagon (Fig. 1B). Body weight was reduced in all STZ mice, with treatment interventions having no impact on this parameter (Fig. 1C). As expected, STZ administration resulted a significant ($P<0.001$) sustained increase in blood glucose levels from day 3 onwards (Fig. 1D). Both desHis^{1}Pro^{4}Glu^{9}-glucagon and desHis^{1}Pro^{4}Glu^{9}-glucagon(Lys^{12}PAL) partially protected ($P<0.05$) against STZ-induced elevations of glucose, but these mice still had increased ($P<0.05$ - $P<0.01$) circulating glucose when compared to HFF control mice (Fig. 1D). In terms of circulating glucagon concentrations, STZ treatment increased ($P<0.001$) circulating glucagon levels in HFF mice on day 18 when compared to lean controls (51.2 ± 13.6 *vs*. 24.3 ± 8.8 pg/ml; respectively), but this effect was fully reversed by both treatment regimens where circulating glucagon was between 19.8–23.4 ± 6.7 pg/ml in these mice on day 18.

Effects of desHis^{1}Pro^{4}Glu^{9}-glucagon or desHis^{1}Pro^{4}Glu^{9}-glucagon(Lys^{12}PAL) on glucose tolerance and insulin sensitivity in HFF-STZ mice

Following an i.p. glucose challenge, glucose levels were significantly lower ($P<0.05$) 15 min post injection in both desHis^{1}Pro^{4}Glu^{9}-glucagon and desHis^{1}Pro^{4}Glu^{9}-glucagon(Lys^{12}PAL) treated HFF-STZ mice when compared to saline controls (Fig. 2A). However, this reduction was not sustained at 30 and 60 min (Fig. 2A), and there was no difference in 0-60 min glucose AUC values between all HFF-STZ groups of mice (Fig. 2B). Glucose-induced insulin secretory responses were almost absent in all HFF-STZ mice, with only control HFF mice displaying any real glucose-induced elevations of insulin concentrations (Fig. 2C,D). The benefits of desHis^{1}Pro^{4}Glu^{9}-glucagon and desHis^{1}Pro^{4}Glu^{9}-glucagon(Lys^{12}PAL) treatment were more prominent following an oral glucose tolerance challenge (Fig. 3A,B). Thus, although individual glucose levels were still elevated in the treatment groups compared to HFF controls (Fig. 3A), 0-60 min AUC values were decreased ($P<0.05$) by desHis^{1}Pro^{4}Glu^{9}-glucagon and desHis^{1}Pro^{4}Glu^{9}-glucagon(Lys^{12}PAL) when compared to STZ-diabetic control mice, and not significantly different from HFF controls (Fig. 3B). However, glucose-induced insulin concentrations were not noticeably amplified by either treatment (Fig. 3C,D). In some agreement with this, the hypoglycaemic action of exogenous insulin was significantly ($P<0.05$ - $P<0.001$) augmented by desHis^{1}Pro^{4}Glu^{9}-glucagon and desHis^{1}Pro^{4}Glu^{9}-glucagon(Lys^{12}PAL), when compared to HFF-STZ or HFF control mice (Fig. 4A,B). Interestingly, STZ administration alone also appeared to enhance ($P<0.05$) peripheral insulin action in HFF mice (Fig. 4A,B). As anticipated, administration of STZ significantly ($P<0.001$) depressed pancreatic insulin content, but 18 days therapy with desHis^{1}Pro^{4}Glu^{9}-glucagon(Lys^{12}PAL) was able to partially reverse ($P<0.001$) this detrimental effect (Fig. 4C). STZ also increased ($P<0.001$) pancreatic glucagon content of HFF mice, but this effect was fully reversed by

Accepted Manuscript published as JOE-22-0106.R2. Accepted for publication: 24-Aug-2022

both desHis^{1}Pro^{4}Glu^{9}-glucagon and desHis^{1}Pro^{4}Glu^{9}-glucagon(Lys^{12}PAL) treatment (Fig. 4D).

Effects of desHis^{1}Pro^{4}Glu^{9}-glucagon or desHis^{1}Pro^{4}Glu^{9}-glucagon(Lys^{12}PAL) on indirect calorimetry and locomotor activity in HFF-STZ mice

Consumption of O_2 was similar in HFF and HFF-STZ mice on day 18, but desHis^{1}Pro^{4}Glu^{9}-glucagon increased ($P<0.001$) this parameter (Fig. 5A,B). Consistent with these findings desHis^{1}Pro^{4}Glu^{9}glucagon also increased CO_2 production ($P<0.01$) in comparison to both HFF and HFF-STZ control mice (Fig. 5C,D). In addition, desHis^{1}Pro^{4}Glu^{9}-glucagon and desHis^{1}Pro^{4}Glu^{9}-glucagon(Lys^{12}PAL) treatment resulted in a significant ($P<0.001$) increase in RER (Fig. 5E,F). Energy expenditure was decreased ($P<0.001$) by STZ administration in HFF mice, which was fully reversed by both GCGR antagonists (Fig. 5G,H). Interestingly, both treatment interventions decreased ($P<0.05$ - $P<0.01$) X beam ambulatory breaks versus HFF-STZ controls during both the light and dark phases (Fig. 6A-C). A similar effect of desHis^{1}Pro^{4}Glu^{9}-glucagon was also noted in terms of Z-beam breaks during the light phase ($P<0.05$), that represent vertical activity levels such as mouse rearing events (Fig. 6D-F). Both peptide treatments had significantly ($P<0.05$ - $P<0.001$) reduced X and Z beam breaks when compared to saline treated HFF controls (Fig. 6A-F).

Discussion

The interplay between pancreatic alpha- and beta-cell signalling is intriguing, with secretions from beta-cells directly inhibiting alpha-cell function, whilst alpha-cells release factors that are stimulatory for beta-cells (English & Irwin 2019; Moede et al. 2020). Coupled with recent awareness that mature beta-cells de-differentiate into alpha-cells (Weir et al. 2013), and that alpha-cells can act as progenitors for functional beta-cells

(Habener & Stanojevic 2012), modulation of alpha-cell activity could hold promise for the treatment of diabetes. Indeed, alpha- to-beta-cell lineage conversion is enhanced in GCGR KO mice (Damond et al. 2016), and more recently human alpha-cells were shown to be capable of reprogramming into glucose-sensitive insulin secreting cells to help ameliorate diabetes in mice (Furuyama et al. 2019). In this regard, inhibition of GCGR signalling has long been considered as a potential means of effectively controlling blood glucose levels (Unger 1978).

In the current study, we employed a high single dose of STZ as an established method to induce beta-cell cytotoxicity and perturb insulin secretory function in HFF mice (Deeds et al. 2011; Millar et al. 2017). Thus, HFF are classically characterised by manifestation of insulin resistance leading to subsequent compensatory beta-cell expansion and hyperinsulinaemia (Ahrén et al. 2010). Notably, saline treated control HFF mice did not present with overt hyperglycaemia, but as expected, glucose intolerance was evident following a glucose challenge likely as a result of dietary-induced insulin resistance (Ahrén et al. 2010). However, hyperglycaemia was clearly apparent in all GCGR antagonist treated HFF-STZ mice by day 18, treatment intervention appeared to delay onset. Indeed, the acylated GCGR analogue partially restored pancreatic insulin concentrations, which may be linked to the more protracted bioactive profile of desHis^{1}Pro^{4}Glu^{9}-glucagon(Lys^{12}PAL) over desHis^{1}Pro^{4}Glu^{9}-glucagon (Franklin et al. 2014). In agreement, GCGR blockade has recently been demonstrated to promote recovery of functional beta-cell mass in diabetic mice (Wang et al. 2021). Regrettably, a technical issue during tissue processing thwarted our efforts to investigate aspects of pancreatic islet morphology, including beta-cell mass and turnover, that would help to validate our observations. Interestingly, the augmented pancreatic insulin content, that was particularly apparent in desHis^{1}Pro^{4}Glu^{9}-glucagon(Lys^{12}PAL) treated HFF-STZ mice, was not matched by prominent improvements of insulin secretory responses or glucose levels. Thus, further investigation of beta-cell

 Accepted Manuscript published as JOE-22-0106.R2. Accepted for publication: 24-Aug-2022

253 secretory function and responsiveness would be required to uncover the relationship
254 between increased insulin stores and translation to more obvious improvements of
255 metabolism in these mice, although improvements in insulin action might also be important
256 in this regard. Circulating and pancreatic glucagon levels were reduced in all GCGR
257 antagonist treated HFF-STZ, which contrasts with observations using small molecule
258 GCGR inhibitors (Mu et al. 2011; 2012), but complements previous work with peptidic
259 GCGR antagonists (Franklin et al. 2014; McShane et al. 2014; O'Harte et al. 2014). This
260 also highlights the improved adverse effect profile of peptidic GCGR antagonists over
261 other methods employed to inhibit GCGR signalling. As such, a rebound hyperglycaemia
262 has been observed on treatment termination with some small molecule GCGR antagonists
263 (Sloop et al. 2004), likely because of their actions to elevate circulating glucagon.

264 Benefits on glucose tolerance were more apparent following an oral as opposed to
265 i.p. glucose challenge in desHis^{1}Pro^{4}Glu^{9}-glucagon and desHis^{1}Pro^{4}Glu^{9}-
266 glucagon(Lys^{12}PAL) treated HFF-STZ mice. In some accord with this, GCGR antagonism-
267 mediated improvements in glycaemic control have been suggested to be dependent on
268 functional GLP-1 receptors (Gu et al. 2010). Indeed, more recent studies have
269 demonstrated that GCGR blockade can promote intestinal L-cell proliferation (Lang et al.
270 2020a) and inhibit L-cell apoptosis (Lang et al. 2020b), leading to elevated GLP-1
271 synthesis and secretion. In agreement, inhibition of the incretin hormone degrading
272 enzyme, dipeptidyl peptidase-4 (DPP-4), improves the effectiveness of GCGR inhibition
273 in diabetic mice (Mu et al. 2011). It has also been suggested that combined GLP-1 receptor
274 activation and GCGR inhibition possesses beneficial actions (Claus et al. 2007).
275 Unfortunately, we were unable to measure circulating GLP-1 concentrations in the current
276 study due to the limited volume of blood that can be withdrawn from mice. However, we
277 have recently shown that combined administration of a peptidic GCGR antagonist, with
278 the well characterised GLP-1 receptor mimetic exendin-4, exerts limited additive metabolic

benefits (Franklin et al. 2022). Thus, activation of receptors for the sister incretin hormone of GLP-1, namely glucose-dependent insulinotropic polypeptide (GIP), may offer a more attractive paradigm in terms of combination therapy with GCGR antagonism (McShane et al. 2016). However, intestinal L-cell number has also been demonstrated to be reduced by STZ administration (Vasu et al. 2015), that could represent another confounding factor in our current observations. Thus, both pancreatic beta-cells and enteroendocrine L-cells appear to have limited antioxidant defence mechanisms (Lenzen 2008; Vasu et al. 2015). Although, in this respect it should be noted that by their very nature, intestinal mucosal cell turnover is rapid, with efficient cellular replacement by differentiating stem cells that arise from intestinal crypts (Roth & Gordon 1990; Schonhoff et al. 2004).

Of note is the improvement of glucose handling in the absence of any real augmentation of insulin concentrations, this being despite elevated pancreatic insulin content in desHis^{1}Pro^{4}Glu^{9}-glucagon(Lys^{12}PAL) treated HFF-STZ mice. It follows that insulin action must be enhanced in these mice, which was indeed apparent following exogenous insulin injection. Similar observations have been made previously following STZ treatment in GCGR KO mice (Lee et al. 2011). In the absence of GCGR signalling, hepatic glucose output and the positive effects of GCGR signalling on basal metabolic rate are also likely to be much reduced (Breton et al. 1983). In good accord with this, in the current study the peptidic GCGR antagonists both decreased physical activity in HFF-STZ mice. However, the ability of desHis^{1}Pro^{4}Glu^{9}-glucagon(Lys^{12}PAL), and particularly desHis^{1}Pro^{4}Glu^{9}-glucagon, to increase energy expenditure does contrast with this notion, but this may simply highlight the plasticity of signalling pathways involved in energy homeostasis (Smith et al. 2018). The slight difference in efficacy between desHis^{1}Pro^{4}Glu^{9}-glucagon and desHis^{1}Pro^{4}Glu^{9}-glucagon(Lys^{12}PAL) in terms of indirect calorimetry data could be related to free versus albumin bound drug, where it is often considered that albumin binding reduces bioactivity of peptides (Miyakawa et al. 2013).

Accepted Manuscript published as JOE-22-0106.R2. Accepted for publication: 24-Aug-2022

However, more detailed pharmacokinetic studies, that are outside the scope of the current investigation, would be required to confirm this. In a similar fashion, there were also slight differences between the effect of both peptides on food and fluid intake. Thus, desHis^{1}Pro^{4}Glu^{9}-glucagon had a mild and transient impact on moderating STZ-induced elevations of feeding, whereas desHis^{1}Pro^{4}Glu^{9}-glucagon(Lys^{12}PAL) exerted more enduring effects to counter increased fluid intake in HFF-STZ mice. Although peptide pharmacodynamic profiles may also be important in this observation, we are unable to discount alterations in the passage of either peptide through the blood–brain barrier and subsequent impact on hypothalamic circuits that regulate energy intake and thirst (Woods 2013).

It is established that glucagon plays an important role in lipid oxidation and metabolism (Galsgaard et al. 2019), and our observed increases in RER evoked by sustained GCGR antagonism likely partly reflects this. Thus, carbohydrate oxidation drives RER to a value closer to 1.0, with fatty acid oxidation reducing this towards 0.7 (Rosenkilde et al. 2010; Purdom et al. 2018). Hyperaminoacidaemia has also been reported following inhibition of GCGR signalling and assessment of plasma amino acids levels would have been interesting in this regard (Richter et al. 2022). Although, the impact of the high fat (45%) background diet, enduring insulin deficiency and small GCGR antagonist-induced changes in food intake and body weight need to be considered in terms of overall effects on carbohydrate metabolism. In that respect, GCGR KO mice are reported to be resistant to high fat feeding induced obesity (Conarello et al. 2007), but the possibility for life-long adaptations in these animals should not be overlooked. However, differences in the magnitude of GCGR signalling annulment between genetic and chemical receptor blockade could also be a factor. Thus, similar to the current setting prolonged treatment with a small molecule GCGR antagonist did not affect body weight in HFF mice (Mu et al. 2011), this being despite increased energy expenditure with desHis^{1}Pro^{4}Glu^{9}-glucagon

and desHis[1]Pro[4]Glu[9]-glucagon(Lys[12]PAL) therapy. The current treatment regimen entailed once daily peptide treatment for 18 days and whether extended dosing periods would lead to more discernible benefits on metabolism in HFF-STZ mice still needs to be established.

In summary, the current study establishes that peptide-based GCGR antagonism exerts notable benefits in obesity-driven forms of diabetes, even in the presence of insulin deficiency. As well as delaying the onset of hyperglycaemia, desHis[1]Pro[4]Glu[9]-glucagon, and particularly desHis[1]Pro[4]Glu[9]-glucagon(Lys[12]PAL), improved glucose handling and insulin action in addition to augmenting pancreatic insulin stores. Our observations further support the promise of peptidic GCGR antagonists as a new class of drugs for management of various forms of diabetes.

 Accepted Manuscript published as JOE-22-0106.R2. Accepted for publication: 24-Aug-2022

Funding

This work was supported by an Invest Northern Ireland Proof-of-Concept grant (PoC106), a Department for the Economy, Northern Ireland PhD studentship and Ulster University Selective Research Funding

Declaration of Interest

There is no conflict of interest that could be perceived as prejudicing the impartiality of the research reported.

Author contributions

NI and FOH conceived/designed and supervised the study. NI, RAL and PRF drafted the manuscript. LMMcS and ZJF and participated in the conduct/data collection and analysis and interpretation of data. All authors revised the manuscript critically for intellectual content and approved the final version of the manuscript.

Data availability statement

The authors declare that the data supporting the findings of this study are available within the article. Any additional raw data supporting the conclusions of this article will be made available by the authors, without undue reservation.

References

Ahrén, J., Ahrén, B., Wierup, N., 2010. Increased β-cell volume in mice fed a high-fat diet: a dynamic study over 12 months. *Islets* **2** 353-356.

Breton, L., Clot, J. P., Baudry, M. 1983. Effects of glucagon on basal metabolic rate and oxidative phosphorylation of rat liver mitochondria. *Horm. Metab Res*. **15** 429-432.

Claus, T. H., Pan, C. Q., Buxton, J. M., Yang, L., Reynolds, J. C., Barucci, N., Burns, M., Ortiz, A. A., Roczniak, S., Livingston, J. N., Clairmont, K. B., Whelan, J. P. 2007. Dual-acting peptide with prolonged glucagon-like peptide-1 receptor agonist and glucagon receptor antagonist activity for the treatment of type 2 diabetes. *J. Endocrinol*. **192** 371-380.

Conarello, S. L., Jiang, G., Mu, J., Li, Z., Woods, J., Zycband, E., Ronan, J., Liu, F., Roy, R. S., Zhu, L., Charron, M. J., Zhang, B. B. 2007. Glucagon receptor knockout mice are resistant to diet-induced obesity and streptozotocin-mediated beta cell loss and hyperglycaemia. *Diabetologia* **50** 142-150.

Damond, N., Thorel, F., Moyers, J.S., Charron, M.J., Vuguin, P.M., Powers, A.C., Herrera, P. L. 2016. Blockade of glucagon signaling prevents or reverses diabetes onset only if residual β-cells persist. *Elife* **19** e13828.

Deeds, M.C., Anderson, J.M., Armstrong, A.S., Gastineau, D.A., Hiddinga, H.J., Jahangir, A., Eberhardt, N.L., Kudva, Y.C. 2011. Single dose streptozotocin-induced diabetes: considerations for study design in islet transplantation models. *Lab Anim*. **45** 131-140.

English, A., Irwin N., 2019. Nonclassical Islet Peptides: Pancreatic and Extrapancreatic Actions. *Clin Med Insights Endocrinol Diabetes*. **12** 1179551419888871.

Farinatti, P., Castinheiras Neto, A.G., Amorim, P.R. 2016. Oxygen consumption and substrate utilization during and after resistance exercises performed with different muscle mass. *Int. J. Exerc. Sci*. **9** 77-88.

Flatt, P. R., Bailey, C. J., 1981. Abnormal plasma glucose and insulin responses in heterozygous lean (ob/+) mice. *Diabetologia* **20** 573-577.

Franklin, Z.J., O'Harte, F.P.M., Irwin, N., 2014. Effects of short-term chemical ablation of glucagon signalling by peptide-based glucagon receptor antagonists on insulin secretion and glucose homeostasis in mice. *Biol. Chem*. **395** 433–442.

Franklin, Z.J., Lafferty, R.A., Flatt, P.R., McShane, L.M., O'Harte, F.P.M., Irwin N., 2022 Metabolic effects of combined glucagon receptor agonism and glucagon-like peptide-1 receptor agonism in high fat fed mice. *Biochimie* **99** 60-67.

Furman, B. L., 2015. Streptozotocin-induced diabetic models in mice and rats. *Curr. Protoc. Pharmacol.* **90** 5.47.1-5.47.20.

Furuyama, K., Chera, S., van Gurp, L., Oropeza, D., Ghila, L., Damond, N., Vethe, H., Paulo, J. A., Joosten, A.M., Berney, T., Bosco, D., Dorrell, C., Grompe, M., Ræder, H., Roep, B. O., Thorel, F., Herrera, P.L., 2019. Diabetes relief in mice by glucose-sensing insulin-secreting human α-cells. *Nature* **56** 43-48.

Galsgaard, K. D., Pedersen, J., Knop, F.K., Holst, J.J., Wewer Albrechtsen, N.J. 2019. Glucagon receptor signalling and lipid metabolism. *Front. Physiol*. **10** 413.

Gu W., Winters K.A., Motani A.S., Komorowski R., Zhang Y., Liu Q., Wu X., Rulifson I.C., Sivits G. Jr., Graham M., Yan H., Wang P., Moore S., Meng T., Lindberg R.A., Véniant M.M. 2010. Glucagon receptor antagonist-mediated improvements in

Accepted Manuscript published as JOE-22-0106.R2. Accepted for publication: 24-Aug-2022

glycemic control are dependent on functional pancreatic GLP-1 receptor. *Am. J. Physiol. Endocrinol. Metab*. **299** E624-632.

Guzman-Perez, A., Pfefferkorn, J.A., Lee, E.C., Stevens, B. D., Aspnes, G. E., Bian, J., Didiuk, M.T., Filipski, K.J., Moore, D., Perreault, C., Sammons ,M.F., Tu, M., Brown, J., Atkinson, K., Litchfield, J., Tan, B., Samas, B., Zavadoski, W.J., Salatto, C.T., Treadway, J., 2013. The design and synthesis of a potent glucagon receptor antagonist with favorable physicochemical and pharmacokinetic properties as a candidate for the treatment of type 2 diabetes mellitus. *Bioorg. Med. Chem. Lett*. **23** 3051-3058.

Habener, J. F., Stanojevic, V., 2012. α-cell role in β-cell generation and regeneration. *Islets* **4** 188-198.

Irwin, N., Franklin, Z.J., O'Harte, F.P.M., 2013 DesHis1Glu9-glucagon-(mPEG) and desHis 1Glu9(Lys30PAL)-glucagon: Long-acting peptide-based PEGylated and acylated glucagon receptor antagonists with potential antidiabetic activity. *Eur. J. Pharmacol*. **709** 43–51.

Kim, W.D., Lee. Y.H., Kim, M.H., Jung, S.Y., Son, W.C., Yoon, S.J., Lee, B.W., 2012. Human monoclonal antibodies against glucagon receptor improve glucose homeostasis by suppression of hepatic glucose output in diet-induced obese mice. *PLoS One* **7** e50954.

Lafferty, R.A., Tanday, N., Flatt, P.R., Irwin, N., 2020. Generation and characterisation of C-terminally stabilised PYY molecules with potential in vivo NPYR2 activity. *Metabolism* **111** 154339.

Lafferty, R.A., O'Harte, F.P.M., Irwin, N., Gault, V.A., Flatt, P.R., 2021. Proglucagon-derived peptides as therapeutics. *Front. Endocrinol*. **12** e689678.

Lang, S., Yang, J., Yang, K., Gu, L., Cui, X., Wei, T., Liu, J., Le, Y., Wang, H., Wei, R., Hong, T., 2020a Glucagon receptor antagonist upregulates circulating GLP-1 level by promoting intestinal L-cell proliferation and GLP-1 production in type 2 diabetes. *BMJ Open Diabetes Res. Care* **8** e001025.

Lang, S., Wei, R., Wei, T., Gu, L., Feng, J., Yan, H., Yang, J., Hong, T., 2020b. Glucagon receptor antagonism promotes the production of gut proglucagon-derived peptides in diabetic mice. *Peptides* **131** 170349.

Lee, Y., Wang, M.Y., Du, X.Q., Charron, M.J., Unger, R.H., 2011. Glucagon receptor knockout prevents insulin-deficient type 1 diabetes in mice. *Diabetes* **60** 391-397.

Lee, Y., Berglund, E.D., Wang, M.Y., Fu, X., Yu, X., Charron, M.J., Burgess, S.C., Unger, R.H., 2012. Metabolic manifestations of insulin deficiency do not occur without glucagon action. *Proc. Natl. Acad. Sci. USA*. **109** 14972-14976.

Lenzen, S., 2008. The mechanisms of alloxan- and streptozotocin-induced diabetes. *Diabetologia* **51** 216-226.

Liang, Y., Osborne, M.C., Monia, B.P., Bhanot, S., Gaarde, W.A., Reed, C., She, P., Jetton, T.L., Demarest, K.T., 2004 Reduction in glucagon receptor expression by an antisense oligonucleotide ameliorates diabetic syndrome in db/db mice. *Diabetes* **53** 410-417.

McShane, L.M., Franklin, Z.J., O'Harte, F.P.M., Irwin, N., 2014. Ablation of glucagon receptor signalling by peptide-based glucagon antagonists improves glucose tolerance in high fat fed mice. *Peptides* **60** 95–101.

McShane, L.M., Irwin, N., O'Flynn, D., Franklin, Z.J., Hewage, C.M., O'Harte, F.P.M., 2016. Glucagon receptor antagonist and GIP agonist combination for diet-induced obese mice. *J Endocrinol*. **229** 319-330.

473 Millar, P., Pathak, N., Parthsarathy, V., Bjourson, A.J., O'Kane, M., Pathak, V., Moffett,
474 R.C., Flatt, P.R., Gault, V.A., 2017. Metabolic and neuroprotective effects of
475 dapagliflozin and liraglutide in diabetic mice. *J. Endocrinol*. **234** 255-267.
476 Miyakawa, N., Nishikawa, M., Takahashi, Y., Ando, M., Misaka, M., Watanabe, Y.,
477 Takakura, Y., 2013. Gene delivery of albumin binding peptide-interferon-gamma
478 fusion protein with improved pharmacokinetic properties and sustained biological
479 activity. *J. Pharm. Sci*. **102** 3110-3118.
480 Moede, T., Leibiger, I.B., Berggren, P.O., 2020. Alpha cell regulation of beta cell function.
481 *Diabetologia* **63** 2064-2075.
482 Morgan, E.S., Tai, L.J., Pham, N.C., Overman, J.K., Watts, L.M., Smith, A., Jung, S.W.,
483 Gajdošík, M., Kršśák, M., Krebs, M., Geary, R.S., Baker, B.F., Bhanot, S., 2019.
484 Antisense inhibition of glucagon receptor by IONIS-GCGRRx improves type 2
485 diabetes without increase in hepatic glycogen content in patients with type 2 diabetes
486 on stable metformin therapy. *Diabetes Care* **42** 585-593.
487 Mu, J., Jiang, G., Brady, E., Dallas-Yang, Q., Liu, F., Woods, J., Zycband, E., Wright, M.,
488 Li, Z., Lu, K., Zhu, L., Shen, X., Sinharoy, R., Candelore, M.L., Qureshi, S.A., Shen,
489 D.M., Zhang, F., Parmee, E.R., Zhang, B.B., 2011. Chronic treatment with a glucagon
490 receptor antagonist lowers glucose and moderately raises circulating glucagon and
491 glucagon-like peptide 1 without severe alpha cell hypertrophy in diet-induced obese
492 mice. *Diabetologia* **54** 2381-2391.
493 Mu, J., Qureshi, S.A., Brady, E.J., Muise, E.S., Candelore, M.R., Jiang, G., Li, Z., Wu,
494 M.S., Yang, X., Dallas-Yang, Q., Miller, C., Xiong, Y., Langdon, R.B., Parmee, E.R.,
495 Zhang, B.B., 2012. Anti-diabetic efficacy and impact on amino acid metabolism of
496 GRA1, a novel small-molecule glucagon receptor antagonist. *PLoS One* **7** e49572.
497 O'Harte, F.P.M., Franklin, Z.J., Rafferty, E.P., Irwin, N., 2013. Characterisation of
498 structurally modified analogues of glucagon as potential glucagon receptor
499 antagonists. *Mol. Cell. Endocrinol*. **381** 26–34.
500 O'Harte, F.P.M, Franklin, Z.J., Irwin, N., 2014. Two novel glucagon receptor antagonists
501 prove effective therapeutic agents in high-fat-fed and obese diabetic mice. *Diabetes*
502 *Obes. Metab*. **16** 1214-1222.
503 O'Harte, F.P.M., Parthsarathy, V., Hogg, C., Flatt, P.R., 2018. Long-term treatment with
504 acylated analogues of apelin-13 amide ameliorates diabetes and improves lipid profile
505 of high-fat fed mice. *PLoS One* **13** e0202350.
506 Okamoto, H., Kim, J., Aglione, J., Lee, J., Cavino, K., Na, E., Rafique, A., Kim, J.H., Harp,
507 J., Valenzuela, D.M., Yancopoulos, G.D., Murphy, A.J., Gromada, J., 2015. Glucagon
508 receptor blockade with a human antibody normalizes blood glucose in diabetic mice
509 and monkeys. *Endocrinology* **156** 2781-2794.
510 Okamoto, H., Cavino, K., Na, E., Krumm, E., Kim, S.Y., Cheng, X., Murphy, A.J.,
511 Yancopoulos, G.D., Gromada, J., 2017. Glucagon receptor inhibition normalizes blood
512 glucose in severe insulin-resistant mice. *Proc. Natl. Acad. Sci. USA*. **114** 2753-2758.
513 Patil, M., Deshmukh, N.J., Patel, M., Sangle, G.V., 2020. Glucagon-based therapy: Past,
514 present and future. *Peptides* **127** e170296.
515 Pettus, J.H., D'Alessio, D., Frias, J.P., Vajda, E.G., Pipkin, J.D., Rosenstock, J.,
516 Williamson, G., Zangmeister, M.A., Zhi, L., Marschke, K.B., 2020. Efficacy and
517 safety of the glucagon receptor antagonist RVT-1502 in type 2 diabetes uncontrolled

Accepted Manuscript published as JOE-22-0106.R2. Accepted for publication: 24-Aug-2022

on metformin monotherapy: A 12-week dose-ranging study. *Diabetes Care* **43** 161-168.

Purdom, T., Kravitz, L., Dokladny, K., Mermier, C., 2018 Understanding the factors that effect maximal fat oxidation. *J. Int. Soc. Sports Nutr*. **15** 3.

Richter, M.M., Galsgaard, K.D., Elmelund, E., Knop, F.K., Suppli, M.P., Holst, J.J., Winther-Sørensen, M., Kjeldsen, S.A.S., Albrechtsen, N.J.W., 2022. The Liver-Alpha Cell Axis in Health and in Disease. *Diabetes* dbi220004. doi: 10.2337/dbi22-0004. Online ahead of print.

Rosenkilde, M., Nordby, P., Nielsen, L.B., Stallknecht, B.M., Helge, J.W. 2010. Fat oxidation at rest predicts peak fat oxidation during exercise and metabolic phenotype in overweight men. *Int. J. Obes*. **34** 871-877.

Roth, K.A., Gordon, J.I., 1990. Spatial differentiation of the intestinal epithelium: analysis of enteroendocrine cells containing immunoreactive serotonin, secretin, and substance P in normal and transgenic mice. *Proc. Natl. Acad. Sci. USA*. **87** 6408-6412.

Schonhoff, S.E., Giel-Moloney, M., Leiter, A.B., 2004. Neurogenin 3-expressing progenitor cells in the gastrointestinal tract differentiate into both endocrine and non-endocrine cell types. *Dev. Biol*. **270** 443-454.

Sloop, K.W., Cao, J.X., Siesky, A.M., Zhang, H.Y., Bodenmiller, D.M., Cox, A.L., Jacobs, S.J., Moyers, J.S., Owens, R.A., Showalter, A.D., Brenner, M.B., Raap, A., Gromada, J., Berridge, B.R., Monteith, D.K., Porksen, N., McKay, R.A., Monia, B.P., Bhanot, S., Watts, L.M., Michael, M.D., 2004. Hepatic and glucagon-like peptide-1-mediated reversal of diabetes by glucagon receptor antisense oligonucleotide inhibitors. *J. Clin. Invest*. **113** 1571-81.

Smith, R. L., Soeters, M. R., Wüst, R., Houtkooper, R. H., 2018. Metabolic flexibility as an adaptation to energy resources and requirements in health and disease. *Endocr. Rev*. **39** 489–517.

Tanday, N., English, A., Lafferty, R.A., Flatt, P.R., Irwin, N., 2021 Benefits of sustained upregulated unimolecular GLP-1 and CCK receptor signalling in obesity-diabetes. *Front. Endocrinol*. **14** 674704.

Unger, R.H., 1978. Role of glucagon in the pathogenesis of diabetes: the status of the controversy. *Metabolism* **27** 1691-709.

Vasu, S., Moffett, R.C., McClenaghan, N.H., Flatt, P.R., 2015. Responses of GLP1-secreting L-cells to cytotoxicity resemble pancreatic β-cells but not α-cells. *J. Mol. Endocrinol*. **54** 91-104.

Wang, M.Y., Dean, E.D., Quittner-Strom, E., Zhu, Y., Chowdhury, K.H., Zhang, Z., Zhao, S., Li, N., Ye, R., Lee, Y., Zhang, Y., Chen, S., Yu, X., Leonard, D.C., Poffenberger, G., Von Deylen, A., McCorkle, S.K., Schlegel, A., Sloop, K.W., Efanov, A.M., Gimeno, R.E., Scherer, P.E., Powers, A.C., Unger, R.H., Holland, W.L., 2021. Glucagon blockade restores functional β-cell mass in type 1 diabetic mice and enhances function of human islets. *Proc. Natl. Acad. Sci. USA*. **118** e2022142118.

Weir, G.C., Aguayo-Mazzucato, C., Bonner-Weir, S., 2013. β-cell dedifferentiation in diabetes is important, but what is it?. *Islets* **5** 233-237.

Woods, S.C., 2013. Metabolic signals and food intake. Forty years of progress. *Appetite* **71** 440-444.

Yang, B., Gelfanov, V.M., Perez-Tilve, D., DuBois, B., Rohlfs, R., Levy, J., Douros, J.D., Finan, B., Mayer, J.P., DiMarchi, R.D., 2021. Optimization of truncated glucagon

564 peptides to achieve selective, high potency, full antagonists. *J. Med. Chem*. **64** 4697–
565 4708.
566
567
568
569
570
571
572
573
574
575
576
577
578
579
580
581
582
583
584
585
586
587
588
589
590

 Accepted Manuscript published as JOE-22-0106.R2. Accepted for publication: 24-Aug-2022

591 **Figure legends**

592 **Figure 1.** Effects of once daily administration of desHis^{1}Pro^{4}Glu^{9}-glucagon or
593 desHis^{1}Pro^{4}Glu^{9}-glucagon(Lys^{12}PAL) (each at 25 nmol/kg bw) for 18 days on cumulative
594 food intake (A), cumulative fluid intake (B), body weight (C) and blood glucose (D) in
595 HFF-STZ mice. Measurements were taken 6 days prior to and throughout the treatment
596 period, at regular intervals. The treatment period is highlighted by the horizontal black bar
597 parallel to x-axis. Values are mean ± SEM (n=8). *p<0.05, **p<0.01, ***p<0.001
598 compared to HFF-STZ saline controls. $^{\Omega}p$<0.05 compared to HFF saline controls.
599
600 **Figure 2.** Effects of once daily administration of desHis^{1}Pro^{4}Glu^{9}-glucagon or
601 desHis^{1}Pro^{4}Glu^{9}-glucagon(Lys^{12}PAL) (each at 25 nmol/kg bw) for 18 days on
602 intraperitoneal glucose tolerance in HFF-STZ mice (18 mmol/kg bw). Blood glucose (A)
603 and associated plasma insulin responses (C) with respective areas under the curves (B,D)
604 are provided. Values are mean ± SEM (n=8). *p<0.05 compared to HFF-STZ saline
605 controls. $^{\Omega}p$<0.05, $^{\Omega\Omega\Omega}p$<0.001 compared to HFF saline controls.
606
607 **Figure 3.** Effects of once daily administration of desHis^{1}Pro^{4}Glu^{9}-glucagon or
608 desHis^{1}Pro^{4}Glu^{9}-glucagon(Lys^{12}PAL) (each at 25 nmol/kg bw) for 18 days on oral glucose
609 tolerance in HFF-STZ mice (18 mmol/kg bw). B Blood glucose (A) and associated plasma
610 insulin responses (C) with respective areas under the curves (B,D) are provided. Values are
611 mean ± SEM (n=8). *p<0.05 compared to HFF-STZ saline controls. $^{\Omega}p$<0.05 compared to
612 HFF saline controls.
613
614 **Figure 4.** Effects of once daily administration of desHis^{1}Pro^{4}Glu^{9}-glucagon or
615 desHis^{1}Pro^{4}Glu^{9}-glucagon(Lys^{12}PAL) (each at 25 nmol/kg bw) for 18 days on insulin
616 sensitivity (A) in HFF-STZ mice, with related area above the curve (B) presented. Insulin

617 was administered by intraperitoneal injection at 5 IU/kg/bw in non-fasted mice.
618 Additionally, effects on pancreatic hormone content were assessed on day 18. Pancreatic
619 glucagon (C) and insulin (D) levels were assessed in excised pancreatic tissue via a
620 commercially available ELISA or in-house radioimmunoassay, respectively. Values are
621 mean ± SEM (n=8). *p<0.05, ***p<0.001 compared to HFF-STZ saline controls. $^{\Omega}p$<0.05,
622 $^{\Omega\Omega\Omega}p$<0.001 compared to HFF saline controls.
623
624 **Figure 5.** Effects of once daily administration of desHis^{1}Pro^{4}Glu^{9}-glucagon or
625 desHis^{1}Pro^{4}Glu^{9}-glucagon(Lys^{12}PAL) (each at 25 nmol/kg bw) for 18 days on O_2
626 consumption (A,B), CO_2 production (C,D), respiratory exchange ratio (RER) (E,F) and
627 energy expenditure (G,H) in HFF-STZ mice. Mice were placed in CLAMS metabolic
628 chambers for 18 h to acclimatise and measurements were obtained over a further 24 h
629 period (12 h dark period as shown by black bar parallel to x-axis) at the end of the treatment
630 period. O_2 consumption and CO_2 production were measured for 30 sec at 25 min intervals
631 (A,C). RER was calculated by dividing VCO_2 by VO_2 (E,F). Energy expenditure was
632 calculated using RER with the following equation: (3.815 + 1.232 x RER) x VO_2 (G).
633 Average energy expenditure is also provided (H), separated into the light (LP) and dark
634 phases (DP). Overall incremental data are presented in panels B,D,F,G, where each data
635 point represents information collected at individual time-points over the 24 h period.
636 Values are mean ± SEM (n=6). **p<0.01, ***p<0.001 compared to HFF-STZ saline
637 controls. $^{\Omega}p$<0.05, $^{\Omega\Omega}p$<0.01, $^{\Omega\Omega\Omega}p$<0.001 compared to HFF saline controls.
638
639 **Figure 6.** Effects of once daily administration of desHis^{1}Pro^{4}Glu^{9}-glucagon or
640 desHis^{1}Pro^{4}Glu^{9}-glucagon(Lys^{12}PAL) (each at 25 nmol/kg bw) for 18 days on locomotor
641 activity in HFF-STZ mice. Mice were placed in CLAMS metabolic chambers for 18 h to
642 acclimatise and measurements were obtained over a further 24 h period (12 h dark period

 Accepted Manuscript published as JOE-22-0106.R2. Accepted for publication: 24-Aug-2022

643 as shown by black bar parallel to x-axis) at the end of the treatment period. Activity counts
644 in X-axis (A-C) and Z-axis (D-F) were recorded at 60 second intervals. Overall incremental
645 data are presented in panels B,C,E,F, where each data point represents information
646 collected at individual time-points over the 24 h period. Values are mean ± SEM (n=6).
647 *p<0.05, **p<0.01 compared to HFF-STZ saline controls. $^{\Omega}p$<0.05, $^{\Omega\Omega}p$<0.01,
648 $^{\Omega\Omega\Omega}p$<0.001 compared to HFF saline controls.

Figure 1

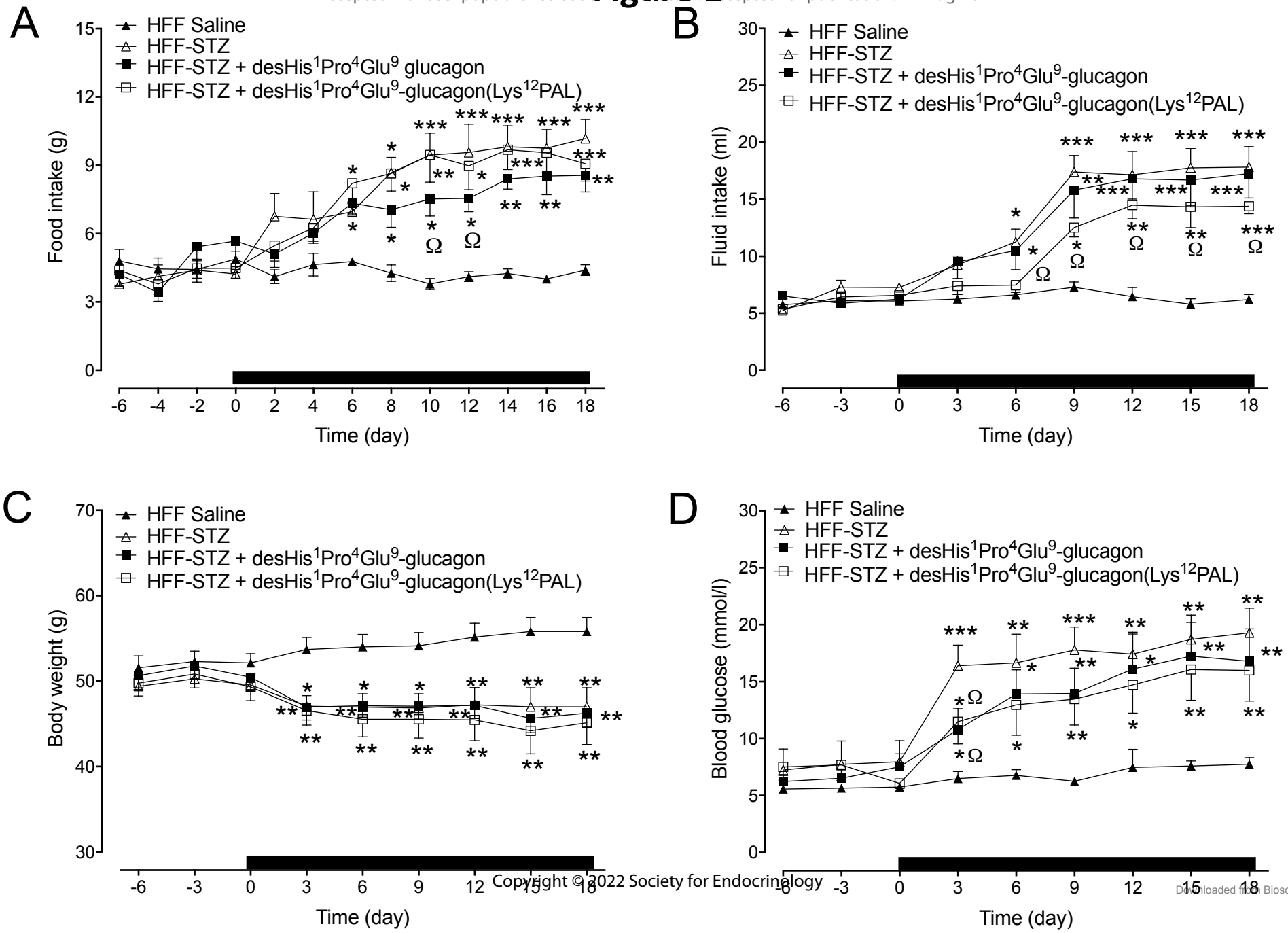

Accepted Manuscript published as JOE-22-0106.R2. Accepted for publication: 24-Aug-2022

Figure 2

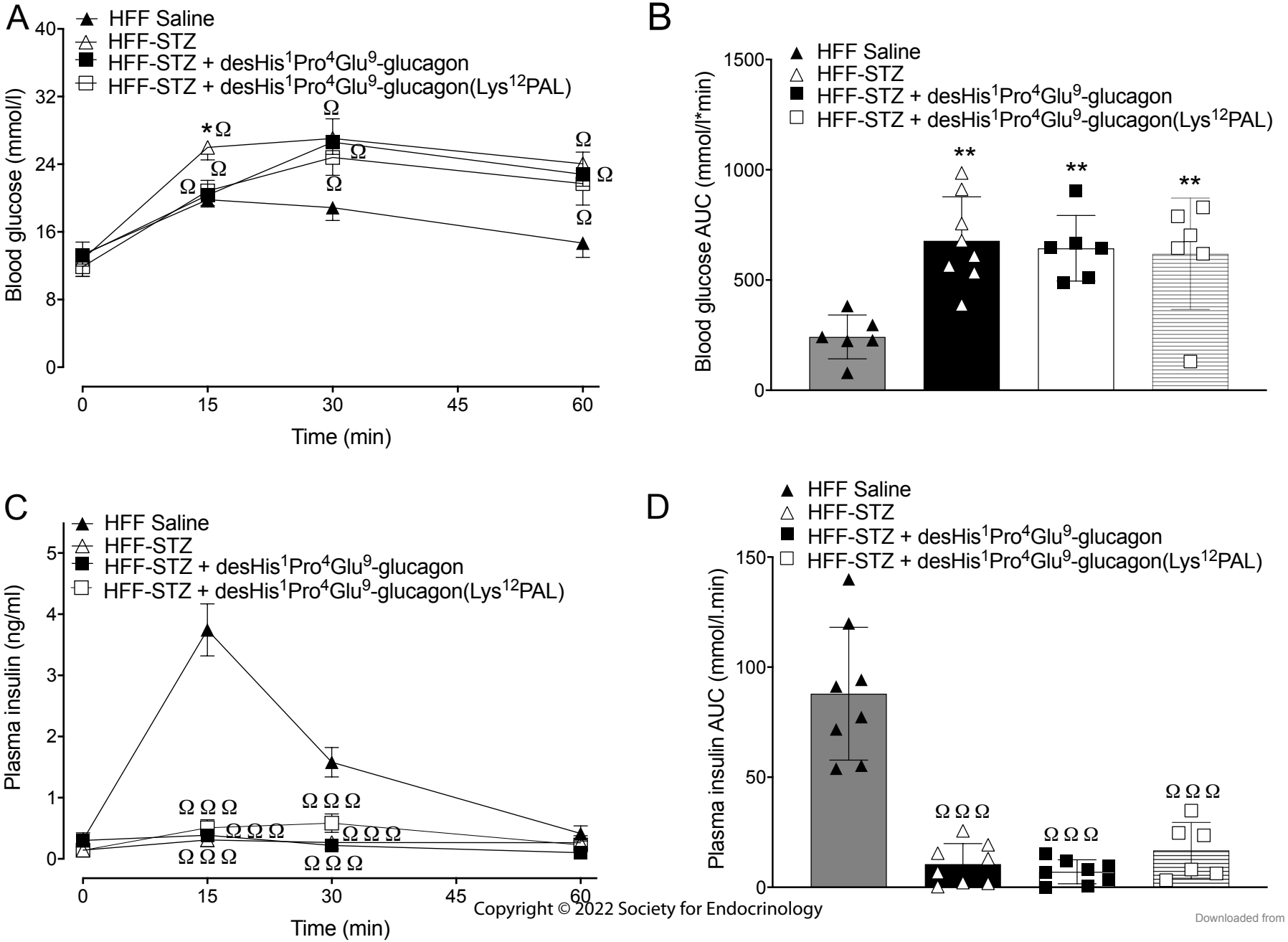

Figure 3

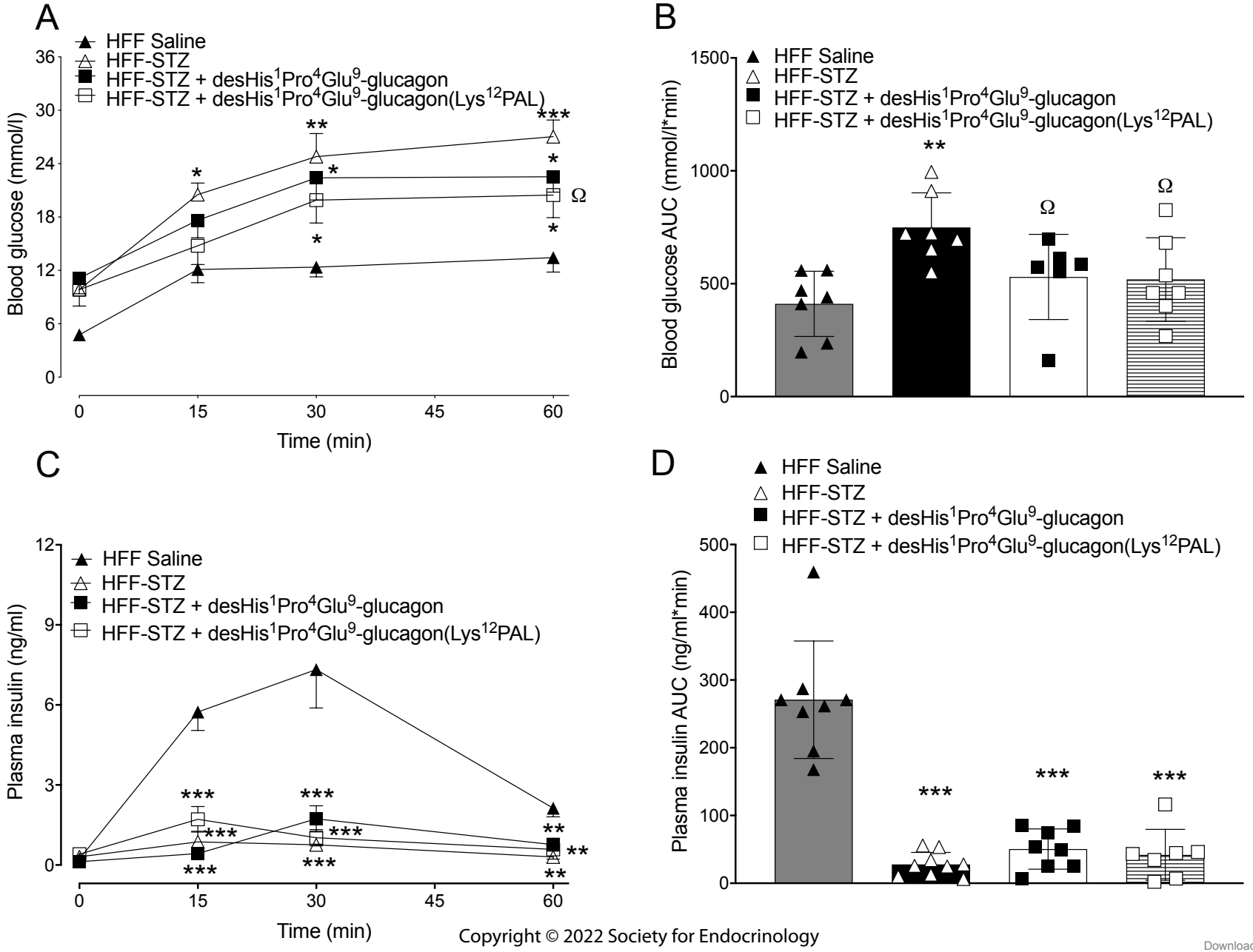

Accepted Manuscript published as JOE-22-0106.R2. Accepted for publication: 24-Aug-2022

Figure 4

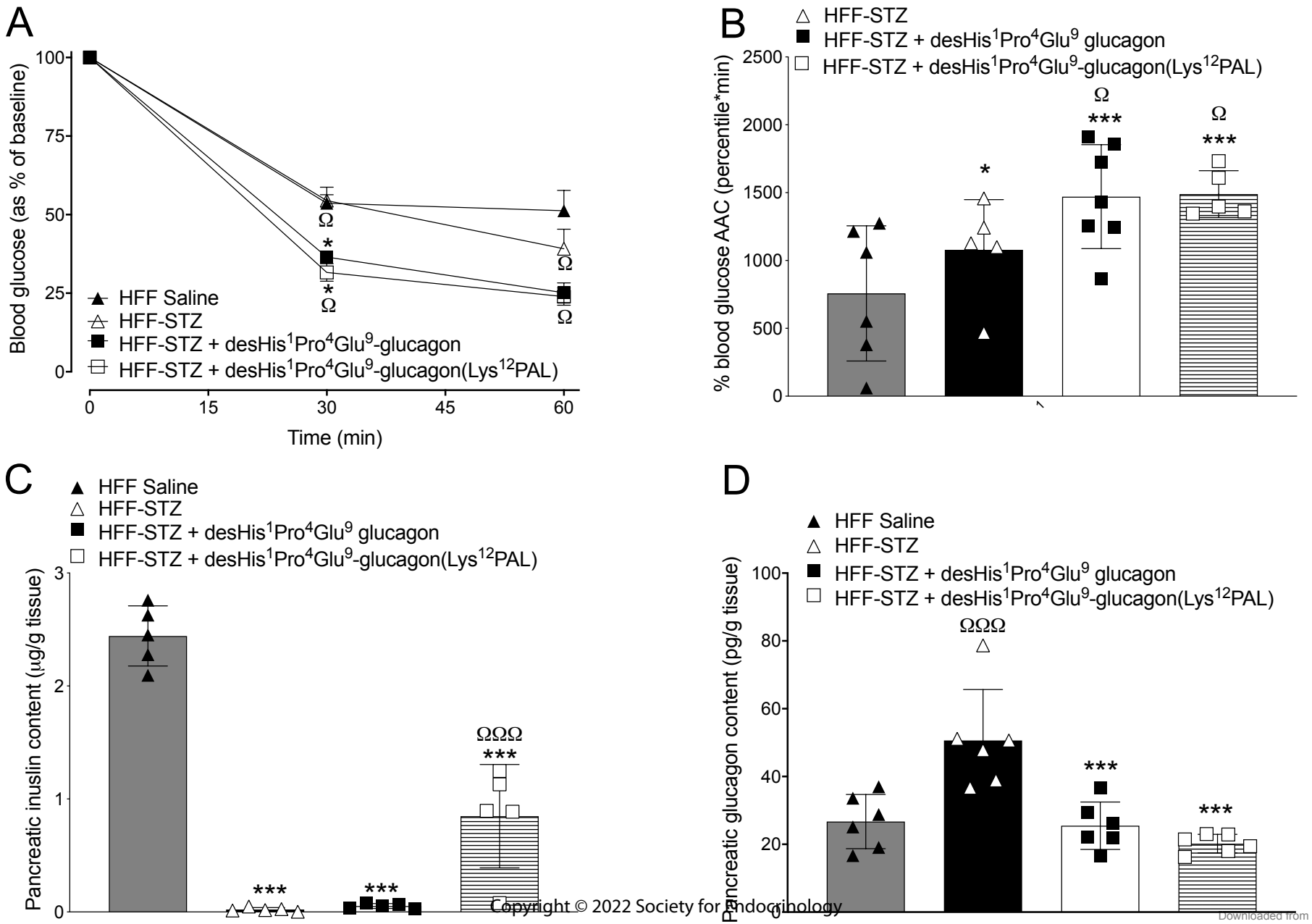

Accepted Manuscript published as JOE-22-0106.R2. Accepted for publication: 24-Aug-2022

Figure 5

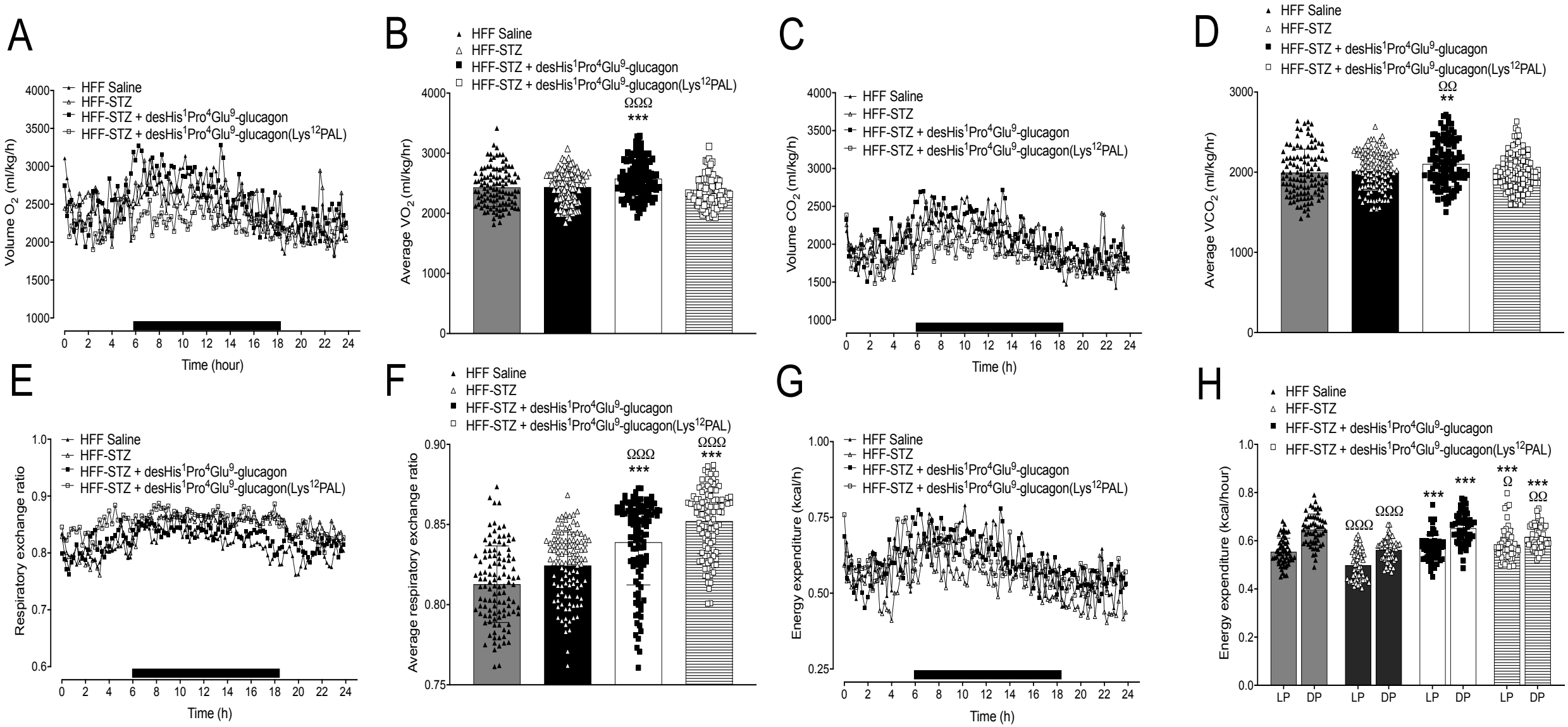

Accepted Manuscript published as JOE-22-0106.R2. Accepted for publication: 24-Aug-2022

Figure 6